Milliarcsecond-scale radio structure of the most distant BL Lac object candidate at redshift 6.57

Frey, S.; Zhang, Y.; Perger, K.; An, T.; Gabányi, K.; Gurvits, L. I.; Hwang, C. Y.; Koptelova, E.; Paragi, Z.; Fogasy, J.

Important note
To cite this publication, please use the final published version (if applicable).
Please check the document version above.

Astronomy & Astrophysics

LETTER TO THE EDITOR

Milliarcsecond-scale radio structure of the most distant BL Lac object candidate at redshift 6.57

S. Frey[1,2,3], Y. Zhang[4,5], K. Perger[1,2], T. An[4,5], K. É. Gabányi[6,7,1,2], L. I. Gurvits[8,9], C.-Y. Hwang[10],
E. Koptelova[10], Z. Paragi[8], and J. Fogasy[1,2]

[1] Konkoly Observatory, HUN-REN Research Centre for Astronomy and Earth Sciences, Konkoly Thege Miklós út 15-17,
1121 Budapest, Hungary
e-mail: frey.sandor@csfk.org
[2] CSFK, MTA Centre of Excellence, Konkoly Thege Miklós út 15-17, 1121 Budapest, Hungary
[3] Institute of Physics and Astronomy, ELTE Eötvös Loránd University, Pázmány Péter sétány 1/A, 1117 Budapest, Hungary
[4] Shanghai Astronomical Observatory, Chinese Academy of Sciences, 80 Nandan Road, Shanghai 200030, PR China
[5] Key Laboratory of Radio Astronomy and Technology, Chinese Academy of Sciences, A20 Datun Road, Chaoyang District,
Beijing 100101, PR China
[6] Department of Astronomy, Institute of Physics and Astronomy, ELTE Eötvös Loránd University, Pázmány Péter sétány 1/A,
1117 Budapest, Hungary
[7] HUN-REN–ELTE Extragalactic Astrophysics Research Group, Eötvös Loránd University, Pázmány Péter sétány 1/A,
1117 Budapest, Hungary
[8] Joint Institute for VLBI ERIC, Oude Hoogeveensedijk 4, 7991 PD Dwingeloo, The Netherlands
[9] Faculty of Aerospace Engineering, Delft University of Technology, Kluyverweg 1, 2629 HS Delft, The Netherlands
[10] Graduate Institute of Astronomy, National Central University, Taoyuan City 32001, Taiwan

ABSTRACT

Context. The existence of accreting supermassive black holes of up to billions of solar masses at early cosmological epochs (in the context of this work, redshifts $z \gtrsim 6$) requires very fast growth rates that are challenging to explain. The presence of a relativistic jet can be a direct indication of activity and accretion status in active galactic nuclei (AGN), constraining the radiative properties of these extreme objects. However, known jetted AGN beyond $z \sim 6$ are still very rare.

Aims. The radio-emitting AGN J2331+1129 has recently been claimed as a candidate BL Lac object at redshift $z = 6.57$ based on its synchrotron-dominated emission spectrum and a lack of ultraviolet or optical emission lines. It is a promising candidate for the highest-redshift blazar known to date. The aim of the observations described here is to support or refute the blazar classification of this peculiar source.

Methods. We performed high-resolution radio interferometric imaging observations of J2331+1129 using the Very Long Baseline Array at 1.6 and 4.9 GHz in February 2022.

Results. The images reveal a compact but slightly resolved, flat-spectrum core feature at both frequencies, indicating that the total radio emission is produced by a compact jet and originates from within a central region of ~10 pc in diameter. While these details are consistent with the radio properties of a BL Lac object, the inferred brightness temperatures are at least an order of magnitude lower than expected for a Doppler-boosted radio jet, which casts doubt on the high-redshift BL Lac identification.

Key words. techniques: interferometric – BL Lacertae objects: individual: J2331+1129 – galaxies: high-redshift –
radio continuum: galaxies

1. Introduction

The most powerful active galactic nuclei (AGN) can be observed from great distances, at redshifts beyond $z = 10$ (Goulding et al. 2023; Bogdán et al. 2023), which correspond to about 3.5% of the present age of the Universe. These objects are powered by material accretion onto the central supermassive black hole (SMBH) of their host galaxy. The existence of black holes reaching billions of solar masses at $z \sim 6$–7 poses a challenge to models describing the formation and early growth of SMBHs (e.g. Volonteri et al. 2021). Recent discoveries of AGN at extremely high redshifts ($z \approx 10$) favour models with massive ($\sim 10^4$–$10^5 M_\odot$) black hole seeds such as those resulting

from direct collapse of gravitationally unstable gas clouds (e.g. Lodato & Natarajan 2006), the merger of or accretion onto primordial black holes (e.g. Cappelluti et al. 2022), and spherically symmetric accretion onto the combined potential of a stellar-mass seed black hole at the centre of a dark matter halo (Sharma & Sharma 2023).

According to the updated catalogue[1] of Perger et al. (2017), the number of currently known $z > 6$ quasars with measured spectroscopic redshift is nearly 300. From these, only 15 sources have been individually detected in radio bands, although many

---

[1] https://cdsarc.cds.unistra.fr/viz-bin/cat/J/other/FrASS/4.9, accessed on 2023 Nov. 14.

of the remaining objects may have some level of weak AGN-related radio emission ([Perger et al. 2019](), [2024]()). Radio-emitting AGN are expected to be found up to $z \approx 15$ in the coming decades thanks to new sensitive radio and optical instruments ([Agudo et al. 2015](); [Ighina et al. 2023](); [Latif et al. 2024]()).

In general, only a minor fraction of quasars (i.e. about 10%; e.g. [Ivezić et al. 2002]()) produce relativistic plasma jets that originate from the close vicinity of the central SMBH. These are strong radio emitters via the synchrotron process of charged particles accelerated to relativistic speeds and moving in magnetic fields. Such sources are important targets for very-long-baseline interferometric (VLBI) observations, which are capable of imaging the radio emission from compact jets down to parsec (pc) scales – more powerful than any other technique in astronomy at present. Radio measurements are not affected by dust obscuration in the young host galaxies and provide unique insight into jet launching and emission. These distant AGN are signposts of the earliest occurrence of SMBH activity in the Universe. Studies of these objects contribute to our understanding of the evolution of jetted AGN and the role jets play in the coevolution of SMBHs and their host galaxies, and may even help evaluate cosmological models.

Blazars form a special class of AGN; their jets are believed to be closely aligned with the line of sight, which means their emission is enhanced by Doppler boosting. About half of the currently known 21 distant radio quasars at $z \geq 5.8$ have been observed (ten objects), and nine have been detected with VLBI ([Frey et al. 2003](), [2005](), [2008](), [2011](); [Momjian et al. 2008](), [2018](), [2021](); [Cao et al. 2014](); [Wang et al. 2017](); [Spingola et al. 2020](); [Zhang et al. 2022](); [Liu et al. 2022]()). Among the latter, the only blazar candidate is PSO J030947.49+271757.31 at $z = 6.10$ ([Spingola et al. 2020]()), based on its prominent one-sided core–jet structure. The other typical $z \gtrsim 6$ VLBI radio sources known to date have a compact but somewhat resolved structure and a steep radio spectrum, indicating unbeamed jet emission and suggesting young age. The double structure of the quasar NDWFS J14276+3312 ($z = 6.12$), with components separated by ~160 pc ([Frey et al. 2008](); [Momjian et al. 2008]()), is reminiscent of compact symmetric objects known to be young ($\lesssim 10^3 - 10^4$ yr) radio sources.

FIRST J233153.20+112952.11 (J2331+1129 hereafter) is a source from the Faint Images of the Radio Sky at Twenty centimeters (FIRST) survey ([Becker et al. 1995]()) catalogue, with a flux density of $S_{1.4\,\text{GHz}} = 1.85$ mJy. This object was recently identified as a high-redshift AGN candidate by cross-matching z_{PS1}-band dropouts from the Panoramic Survey Telescope and Rapid Response System 1 (Pan-STARRS1, [Chambers et al. 2016]()) with FIRST radio sources ([Koptelova & Hwang 2022]()). The source has counterparts in the near- and mid-infrared, as well as in other radio surveys. Its radio spectrum is flat within a relatively narrow range of frequencies, between the observed 888 MHz and 3 GHz (spectral index $\alpha = -0.01 \pm 0.06$, defined here as $S \propto \nu^\alpha$, where ν is the frequency), with flux densities around 2 mJy. The optical-to-radio spectral energy distribution of J2331+1129 is dominated by the synchrotron emission of the jet and closely resembles those of BL Lac objects. The non-thermal ultraviolet/optical continuum has a spectral index of $\alpha_{\text{opt}} = 1.43 \pm 0.23$. The source appears variable in near-infrared – and possibly in radio as well – on timescales of months to years in the observer's frame. The observed near-infrared spectrum shows no detected emission lines ([Koptelova & Hwang 2022]()). Its redshift was estimated based on the Gunn–Peterson trough ([Gunn & Peterson 1965]()) found at the wavelength $\lambda = 0.921$ μm, giving a lower redshift limit of $z = 6.57$. The observed properties

together suggest that this AGN belongs to a subclass of blazars, BL Lac objects, and therefore might be the highest-redshift BL Lac discovered to date. Notably, no BL Lac objects have been found so far beyond $z = 4$ ([Koptelova & Hwang 2022]()).

VLBI imaging observations with milliarcsec (mas) resolution are essential for verifying the truly compact radio structure and the high brightness temperature expected for a relativistically beamed jet of a BL Lac object. Here we report on our dual-frequency (1.6 and 4.9 GHz) observations of J2331+1129 with the U.S. National Radio Astronomy Observatory (NRAO) Very Long Baseline Array (VLBA). Throughout this Letter, we assume a flat Λ cold dark matter cosmological model with Hubble constant $H_0 = 70$ km s^{-1} Mpc^{-1}, matter density parameter $\Omega_{\text{m}} = 0.3$, and vacuum energy density parameter $\Omega_\Lambda = 0.7$. In this model, the luminosity distance at $z = 6.57$ is $D_{\text{L}} = 64.119$ Gpc, the angular scale is 5.425 pc mas^{-1}, and the age of the Universe is 813 Myr ([Wright 2006]()).

2. Observations and data reduction

We conducted observations of J2331+1129 with the VLBA at the central frequencies of 1.6 and 4.9 GHz on 2022 Feb 1 and 4, respectively (project code: BF132, P.I.: S. Frey). The experiment was performed in phase-referencing mode ([Beasley & Conway 1995]()) using J2330+1100 as a phase calibrator. This source is listed in the third edition of the International Celestial Reference Frame (ICRF3, [Charlot et al. 2020]()) and its angular separation from the target is 0°.59. Both experiment segments lasted for 4 h and recorded data in left and right circular polarisations. The observing time spent on the target, J2331+1129, was 165 min in each segment. For the lower frequency band, the observations were conducted in two intermediate frequency channels (IFs) around 1.4 and 1.7 GHz. The data rate was 2 Gbps. At 4.9 GHz, the data rate was 4 Gbps with four IFs. In both experiment segments, the bandwidth was 128 MHz per IF and polarisation. The raw data recorded at each VLBA telescope were correlated at the DiFX correlator ([Deller et al. 2011]()) in Socorro (New Mexico, USA) with 2 s integration time.

The VLBA data were calibrated in the standard way in the NRAO Astronomical Image Processing System package (Aips, [Greisen 2003]()). The appropriate tasks and procedures were used to correct for the dispersive ionospheric delays based on models from Global Navigation Satellite Systems data, and the accurate Earth orientation parameters. After digital sampling corrections, we performed manual phase calibration to remove instrumental delays using a short 1min scan spent on the secondary calibrator source J2327+0940 also scheduled in the experiment. Bandpass correction was performed using the same section of data. Amplitude calibration was then carried out using antenna-based system temperatures and gain curves supplied along with the correlated visibility data. Finally, global fringe-fitting was attempted for the bright sources observed, J2330+1100, J2327+0940, and the fringe-finder 3C 454.3. The phase, delay, and delay-rate solutions were applied to the respective source data.

The calibrated single-source visibility files were then exported to the Caltech Difmap program ([Shepherd 1997]()) for hybrid mapping. The procedure started with several iterations of Clean image decomposition and phase self-calibration. To begin the amplitude and phase self-calibration, the overall antenna gain correction factors were determined. In a few cases, when gain corrections exceeded ±5%, those values were fed back into Aips to refine the amplitude calibration.

Fringe-fitting was then repeated for the phase-reference calibrator J2330+1100 in Aips. Now the Clean image of the source
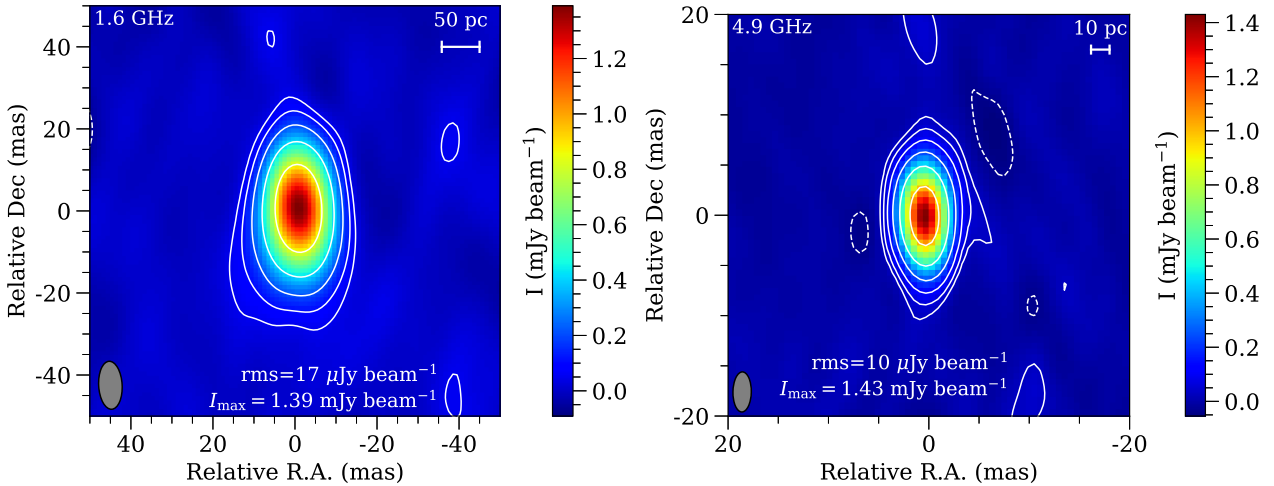
Fig. 1. Naturally weighted VLBA images of J2331+1129 at 1.6 GHz *(left)* and 4.9 GHz *(right)*. The intensity colour scales are displayed on the right-hand side of the panels. The lowest contours start at $\pm 3\sigma$ rms noise, and the positive levels increase by a factor of 2. Image rms and peak intensity values are shown at the bottom of the panels, and the elliptical Gaussian restoring beams are shown in the lower left corners. The beam sizes are 11.7 mas × 5.7 mas and 4.0 mas × 1.8 mas (FWHM), with major axis position angles of 3°2 and −1°0 (measured from north through east) at 1.6 and 4.9 GHz, respectively.

obtained in DIFMAP was also used as an input to account for a potential small phase contribution of the source structure. The solutions obtained for the calibrator were then interpolated to the target source.

During imaging of J2331+1129 in DIFMAP, we did not attempt any self-calibration because of the weakness of the target source. Radio emission was clearly detected both at 1.6 and 4.9 GHz. However, the source position was offset by ~0.1″ in both right ascension (RA) and declination (Dec) with respect to the a priori pointing position. To minimise smearing effects, we repeated the calibration steps in AIPS but with the target source coordinates shifted to the newly determined accurate position.

3. Results and discussion

Results of the CLEAN imaging of J2331+1129 are displayed in Fig. 1. We find that the source is compact but slightly resolved at both observing frequencies. To characterise its brightness distribution quantitatively, we fitted circular Gaussian model components directly to the interferometric visibility data in DIFMAP. At 1.6 GHz, the flux density is $S_{1.6\,\mathrm{GHz}} = (1.8 \pm 0.2)$ mJy and the full width at half maximum (FWHM) of the component diameter is $\theta_{1.6\,\mathrm{GHz}} = (3.67 \pm 0.05)$ mas. At 4.9 GHz, the parameters of the circular Gaussian component that adequately describe the source are $S_{4.9\,\mathrm{GHz}} = (1.6 \pm 0.2)$ mJy and $\theta_{4.9\,\mathrm{GHz}} = (0.68 \pm 0.01)$ mas. The fitted component sizes exceed the minimum resolvable angular size of the interferometer (Kovalev et al. 2005). These angular sizes correspond to a linear extent of about (4−20) pc if we assume that the source is at $z = 6.57$.

The accurate coordinates of the target source calculated by finding the 4.9 GHz image brightness peak position with the AIPS command MAXFIT are RA = $23^\mathrm{h}31^\mathrm{m}53{.}^\mathrm{s}21007$ and Dec = $11°29'52{.}''0089$. The estimated uncertainty of 0.2 mas in both coordinates is dominated by the effect arising from the angular distance of the phase-reference calibrator source (cf. Chatterjee et al. 2004; Rioja & Dodson 2020). The position determined at 1.6 GHz is slightly less accurate but the coordinates are consistent with the above values within the errors.

Based on the fitted flux densities, the radio spectrum of the ~10 pc scale structure is flat ($\alpha_{\mathrm{pc}} = -0.11$), similar

to what is known from the total flux density measurements (Koptelova & Hwang 2022). Irrespective of whether or not we consider a ~10−20% coherence loss (Martí-Vidal et al. 2010) in phase-referenced observations, the measured flux densities are a good match to those obtained with lower-resolution connected-element interferometers, indicating that the total radio emission of J2331+1129 is mostly confined to the region imaged with VLBI.

For comparison with other high-redshift radio AGN, we calculated the 1.4 GHz rest-frame radio power as $P = 4\pi S_{1.4\,\mathrm{GHz}}D_\mathrm{L}^2(1+z)^{-\alpha-1}$. The high value of $P = 1.4 \times 10^{26}$ W Hz^{-1} suggests that the emission originates from a powerful AGN (see Perger et al. 2019, and references therein), provided that the source is indeed at such a high redshift.

The brightness temperatures were calculated as

$$T_\mathrm{b} = 1.22 \times 10^{12}(1+z)\frac{S_\nu}{\nu^2\theta^2}\ \mathrm{K},\qquad(1)$$

where the flux density S_ν is measured in Jy, the observing frequency ν in GHz, and the circular Gaussian component diameter θ (FWHM) in mas. The values ($T_\mathrm{b} \approx 5 \times 10^8$ K at 1.6 GHz and $T_\mathrm{b} \approx 1.5 \times 10^9$ K at 4.9 GHz) also confirm the non-thermal nature of the radio emission that originates from AGN activity. This conclusion is so robust that it would hold true even if $z = 0$, because brightness temperatures exceeding $T_\mathrm{b} \sim 10^5$ K cannot be attributed to star-forming activity in the host galaxy (Condon 1992).

Even the higher measured brightness temperature for J2331+1129 is an order of magnitude below the equipartition limit of $T_\mathrm{b,eq} \approx 5 \times 10^{10}$ K (Readhead 1994) when the energy density in the radiating particles matches that of the magnetic field. This is conventionally assumed as the intrinsic value in the core region of the jet. In our case, the Doppler boosting factor, that is, the ratio of measured and intrinsic brightness temperatures, $\delta = T_\mathrm{b}/T_\mathrm{b,int} = T_\mathrm{b}/T_\mathrm{b,eq}$, is smaller than 1. This would indicate that the radio emission is not relativistically boosted, contrary to what one would expect for a powerful blazar jet pointing nearly to the line of sight. Even considering a somewhat lower intrinsic brightness temperature of $T_\mathrm{b,int} \approx 3 \times 10^{10}$ K (Homan et al. 2006), which is the average value found in samples of powerful

jetted AGN in their median-low state (i.e. not in outburst when brightness temperatures can reach order-of-magnitude-higher values), δ remains well below unity.

Based on a large sample of jetted AGN (mostly blazars) studied with VLBI, Cheng et al. (2020) found that brightness temperatures are generally frequency dependent, reaching their maximum at the emitted (rest-frame) frequency $\nu_{em} \approx 6.8$ GHz. If the redshift of J2331+1129 is indeed extremely high, the observed $\nu = 4.9$ GHz frequency corresponds to $\nu_{em} = \nu(1 + z) = 37$ GHz in the expanding Universe. According to the phenomenological dependence derived by Cheng et al. (2020), the maximum brightness temperature of the source could then be a factor of $\sim 4-5$ higher than what we measured at $\nu = 4.9$ GHz, which would equate to $\sim 5 \times 10^9$ K. In any case, this is still not as high as expected having observed Doppler-boosted emission in the J2331+1129 jet. However, we note that the core brightness temperatures (or lower limits) of the only other claimed blazar candidate known to date at $z > 6$, namely PSO J030947.49+271757.31, are also on the order of $T_b \sim 10^8$ K (Spingola et al. 2020). On the other hand, for the previously known second-most distant blazar, J0906+6930 ($z = 5.47$), the brightness temperature measured with VLBI (3×10^{11} K) clearly exceeds the equipartition limit (An et al. 2020).

The flat section of the radio spectrum of J2331+1129 around $\nu \gtrsim 1$ GHz (see also Koptelova & Hwang 2022), although not yet sampled in a sufficiently broad range of frequencies, could possibly be interpreted as similar to those of gigahertz-peaked spectrum (GPS) radio sources (e.g. O'Dea & Saikia 2021, and references therein). However, GPS sources typically have more extended mas-scale radio structure, that is, within about 500 pc in size (O'Dea & Saikia 2021). Indeed, a high-redshift GPS source recently studied with VLBI, J1606+3124 ($z = 4.56$), shows a relatively compact (~ 70 pc) triple structure (An et al. 2022), much different from the single component (< 20 pc) we see in J2331+1129.

We note that, assuming $z = 6.57$ for our source, the observed ~ 1 GHz frequency range translates to above 5 GHz, where turnover frequencies are characteristic of high-frequency peaker (HFP) sources (O'Dea & Saikia 2021). Typically both HFPs and GPS sources have less compact structures that blazar core-jets. However, HFP and blazar properties are not necessarily mutually exclusive. A good example is J0906+6930 ($z = 5.47$), which has a peaked broad-band radio spectrum with a turnover frequency of $\nu_{em} \approx 40$ GHz (Coppejans et al. 2017; Zhang et al. 2017) but also very compact Doppler-boosted jet emission (An et al. 2020). Future flux density measurements of J2331+1129 in a frequency range wider than available at present (as in the sample of $z > 5$ radio AGN by Shao et al. 2022) would provide decisive information about the possible HFP nature of this source. At present, the previous low-resolution data and our recent VLBI data indicate that the radio spectrum of J2331+1129 is likely flat between the observed 888 MHz and 4.9 GHz, as expected for blazars. The currently available data do not show evidence for a spectral turnover at gigahertz frequencies.

4. Summary and conclusions

The redshift of $z = 6.57$ for the radio-emitting AGN J2331+1129 was inferred from the shape of the near-infrared continuum spectrum (Koptelova & Hwang 2022). The lack of identifiable emission lines, as well as the flat radio spectrum in the observed GHz range, the spectral energy distribution, and the indication of variability, led Koptelova & Hwang (2022) to classify the source as a candidate BL Lac object, by far the most distant known to date.

However, as the redshift determination is based on the location of the break in the continuum spectrum and not on emission lines, the value should be considered approximate.

We performed high-resolution radio interferometric observations with the VLBA to reveal whether or not there is a compact core–jet structure in J2331+1129. Nearly simultaneous dual-frequency (1.6- and 4.9-GHz) imaging shows a compact, flat-spectrum radio core whose flux density matches the total flux density, indicating that the entire radio emission is confined within ~ 20 pc. Via traditional nodding-style phase referencing to a nearby ICRF3 radio quasar, we precisely determined the astrometric position of the source with sub-mas accuracy.

The inferred maximum brightness temperature is about 5×10^9 K, confirming that this is an AGN source but providing no clear evidence for Doppler-boosted radio jet emission. This leaves the BL Lac identification of the source unconfirmed. Comparing the brightness temperature of J2331+1129 with those of other high-redshift ($z \gtrsim 6$) blazars may allow confirmation of the nature of this object. However, currently the sample of known sources with similar properties is very small. It is possible that the observed jet properties in extremely distant radio sources differ from those at lower redshifts because of yet poorly understood evolutionary and environmental effects. The rarity of $z \gtrsim 6$ blazars means that each new discovery and study significantly adds to our understanding of the behaviour of jetted SMBHs in the early Universe. Observational limitations could also play a role, as phase-referenced VLBI observations of weak radio sources may only provide an upper limit on the resolved source size, and therefore a lower limit to the brightness temperature.

To verify the BL Lac nature of J2331+1129, sensitive VLBI observations at higher frequencies and therefore higher resolution might prove useful. Also, densely time-sampled total flux density monitoring could possibly reveal rapid variations indicative of high brightness temperature. Finally, it cannot be excluded that the source is a misidentified BL Lac object and/or is not at extremely high redshift. This should be tested in the future with sensitive spectroscopic observations to look for emission lines and possibly re-evaluate the redshift.

References

Agudo, I., Boettcher, M., Falcke, H. D. E., et al. 2015, in Advancing Astrophysics with the Square Kilometre Array (AASKA14), 93
An, T., Mohan, P., Zhang, Y., et al. 2020, Nat. Commun., 11, 143
An, T., Wang, A., Zhang, Y., et al. 2022, MNRAS, 511, 4572
Beasley, A. J., & Conway, J. E. 1995, in Very Long Baseline Interferometry and the VLBA, eds. J. A. Zensus, P. J. Diamond, & P. J. Napier, ASP Conf. Ser., 82, 327
Becker, R. H., White, R. L., & Helfand, D. J. 1995, ApJ, 450, 559
Bogdán, Goulding, A.D., Natarajan, P., et al. 2023, Nat. Astron., http://dx.doi.org/10.1038/s41550-023-02111-9
Cao, H. M., Frey, S., Gurvits, L. I., et al. 2014, A&A, 563, A111
Cappelluti, N., Hasinger, G., & Natarajan, P. 2022, ApJ, 926, 205

Chambers, K. C., Magnier, E. A., Metcalfe, N., et al. 2016, arXiv e-prints [arXiv:1612.05560]

Charlot, P., Jacobs, C. S., Gordon, D., et al. 2020, A&A, 644, A159

Chatterjee, S., Cordes, J. M., Vlemmings, W. H. T., et al. 2004, ApJ, 604, 339

Cheng, X. P., An, T., Frey, S., et al. 2020, ApJS, 247, 57

Condon, J. J. 1992, ARA&A, 30, 575

Coppejans, R., van Velzen, S., Intema, H. T., et al. 2017, MNRAS, 467, 2039

Deller, A. T., Brisken, W. F., Phillips, C. J., et al. 2011, PASP, 123, 275

Frey, S., Gurvits, L. I., Paragi, Z., & É. Gabányi, K. 2008, A&A, 484, L39

Frey, S., Mosoni, L., Paragi, Z., & Gurvits, L. I. 2003, MNRAS, 343, L20

Frey, S., Paragi, Z., Mosoni, L., & Gurvits, L. I. 2005, A&A, 436, L13

Frey, S., Paragi, Z., Gurvits, L. I., Gabányi, K. É., & Cseh, D. 2011, A&A, 531, L5

Goulding, A. D., Greene, J. E., Setton, D. J., et al. 2023, ApJ, 955, L24

Greisen, E. W. 2003, in Information Handling in Astronomy – Historical Vistas, ed. A. Heck, Astrophys. Space Sci. Lib., 285, 109

Gunn, J. E., & Peterson, B. A. 1965, ApJ, 142, 1633

Homan, D. C., Kovalev, Y. Y., Lister, M. L., et al. 2006, ApJ, 642, L115

Ighina, L., Caccianiga, A., Moretti, A., et al. 2023, MNRAS, 519, 2060

Ivezić, Ž., Menou, K., Knapp, G. R., et al. 2002, AJ, 124, 2364

Koptelova, E., & Hwang, C.-Y. 2022, ApJ, 929, L7

Kovalev, Y. Y., Kellermann, K. I., Lister, M. L., et al. 2005, AJ, 130, 2473

Latif, M. A., Whalen, D. J., & Mezcua, M. 2024, MNRAS, 527, L37

Liu, Y., Wang, R., Momjian, E., et al. 2022, ApJ, 939, L5

Lodato, G., & Natarajan, P. 2006, MNRAS, 371, 1813

Martí-Vidal, I., Ros, E., Pérez-Torres, M. A., et al. 2010, A&A, 515, A53

Momjian, E., Carilli, C. L., & McGreer, I. D. 2008, AJ, 136, 344

Momjian, E., Carilli, C. L., Bañados, E., Walter, F., & Venemans, B. P. 2018, ApJ, 861, 86

Momjian, E., Bañados, E., Carilli, C. L., Walter, F., & Mazzucchelli, C. 2021, AJ, 161, 207

O'Dea, C. P., & Saikia, D. J. 2021, A&ARv, 29, 3

Perger, K., Frey, S., & Gabányi, K. É. 2024, MNRAS, 527, 3436

Perger, K., Frey, S., Gabányi, K. É., & Tóth, L. V. 2017, Front. Astron. Space Sci., 4, 9

Perger, K., Frey, S., Gabányi, K. É., & Tóth, L. V. 2019, MNRAS, 490, 2542

Readhead, A. C. S. 1994, ApJ, 426, 51

Rioja, M. J., & Dodson, R. 2020, A&ARv, 28, 6

Shao, Y., Wagg, J., Wang, R., et al. 2022, A&A, 659, A159

Sharma, R., & Sharma, M. 2023, arXiv e-prints [arXiv:2310.06898]

Shepherd, M.C. 1997, in Astronomical Data Analysis Software and Systems VI, eds. G. Hunt, & H. Payne, ASP Conf. Ser., 125, 77

Spingola, C., Dallacasa, D., Belladitta, S., et al. 2020, A&A, 643, L12

Volonteri, M., Habouzit, M., & Colpi, M. 2021, Nat. Rev. Phys., 3, 732

Wang, R., Momjian, E., Carilli, C. L., et al. 2017, ApJ, 835, L20

Wright, E. L. 2006, PASP, 118, 1711

Zhang, Y., An, T., Frey, S., et al. 2017, MNRAS, 468, 69

Zhang, Y., An, T., Wang, A., et al. 2022, A&A, 662, L2